A spring in performance: silica nanosprings boost enzyme immobilization in microfluidic channels

Donya Valikhani,[‡] *Juan M. Bolivar,*[‡] *Martina Viefhues,*[§,†] *David N. McIlroy,*[⊥] *Elwin X. Vrouwe*[§] *and Bernd Nidetzky*[*,‡,¶]

[‡] Institute of Biotechnology and Biochemical Engineering, Graz University of Technology, NAWI Graz, Petersgasse 12, 8010 Graz, Austria

[§] Micronit Microtechnologies B.V., Colloseum 15, 7521 PV Enschede, The Netherlands

[⊥] Department of Physics, Oklahoma State University, Stillwater, OK, 74078-3072, United States

[¶] Austrian Centre of Industrial Biotechnology, Petersgasse 14, 8010 Graz, Austria

KEYWORDS: surface modification, silica nanosprings, microreactor, biocatalysis, enzyme immobilization

ABSTRACT

Enzyme microreactors are important tools of miniaturized analytics and have promising applications in continuous biomanufacturing. Fundamental problem of their design is that plain microchannels without extensive static internals, or packings, offer limited exposed surface area for immobilizing the enzyme. To boost the immobilization in a manner broadly applicable to enzymes, we coated borosilicate microchannels with silica nanosprings and attached the enzyme, sucrose phosphorylase, via a silica-binding module genetically fused to it. We showed with confocal fluorescence microscopy that the enzyme was able to penetrate the ~70-μm thick nanospring layer and became distributed uniformly in it. Compared with the plain surface, the activity of immobilized enzyme was enhanced 4.5-fold upon surface coating with nanosprings and further increased up to 10-fold by modifying the surface of the nanosprings with sulfonate groups. Operational stability during continuous-flow biocatalytic synthesis of α-glucose 1-phosphate was improved by a factor of 11 when the microreactor coated with nanosprings was used. More than 85% of the initial conversion rate was retained after 840 reactor cycles performed with a single loading of enzyme. By varying the substrate flow rate, the microreactor performance was conveniently switched between steady states of quantitative product yield (50 mM) and optimum productivity (19 mM min^{-1}) at a lower product yield of 40%. Surface coating with silica nanosprings thus extends the possibilities for enzyme immobilization in microchannels. It effectively boosts the biocatalytic function of a microstructured reactor limited otherwise by the solid surface available for immobilizing the enzyme.

1. INTRODUCTION

Continuous-flow microfluidics is the key enabling technology for many important applications, from the Lab-on-the-Chip implementations in analytics, cell biology and medicine[1-5] to the advanced tools of microprocess engineering in chemistry and biotechnology.[5-13] Microfluidic biocatalysis plays a central role in biochips for DNA sequencing, proteomic analysis and clinical metabolite detection.[11,14,15] It has furthermore aroused significant interest for use in various flow chemistry applications. The idea in general is that by combining the high selectivity of enzymes with the efficient fluidics of a microstructured flow reactor, the performance characteristics of certain chemical transformations can be enhanced substantially. Fundamental problem of all microfluidic biocatalysis in continuous flow is, however, that irrespective of the enzyme's actual use for sample pretreatment, analytical detection or organic synthesis, the enzyme must be applied in a form that prevents it from being washed away.[10-13,16] Immobilizing the enzyme on the wall surface of the microchannels presents the most straightforward solution.[10,17-22] Doing so, however, demands a strongly integrated development of the microfluidic system considered. The flow channels must be designed to accommodate a suitable amount of active enzyme immobilized on their solid walls, since the conversion rate scales directly with that amount.[19,20,23-24] The contrast to enzyme immobilization in conventional reactors is immediately noted. Bulk-scale immobilization is usually done on porous particles and so represents a task of the overall bioprocess development that is pursued somewhat independently of the actual bioreactor design.[25-29]

Microchannel design for efficient immobilization needs to conjoin aspects of overall geometry and internal structure of the microchannels with those of the material used for microfabrication. The core problem is that plain microchannels, lacking extensive static internals or packings, offer only

a limited amount of solid surface for immobilizing the enzyme. Because microparticle packings result in large pressure drops, and static internals alter the liquid flow pattern[12,30] usually more than they help increasing the surface area, enhancement of the enzyme-accessible surface directly on the microchannel walls remains as the most promising option. Among the materials widely used in microfluidics, silica has excellent properties, including high compatibility with enzymes, substrates and solvents.[26] Immobilization technology based on silica-binding modules (SBM) enables convenient immobilization of enzymes on plain silica (e.g., borosilicate glass). The SBM is a small three-helical protein, often referred to also as Z_{basic2}, that is highly positively charged on one protein face due to multiple Arg residues pointing outward.[19-21,27] The SBM is genetically fused to the enzyme of interest and the resulting enzyme chimera becomes attached to underivatized silica surfaces via the SBM. Under conditions in which the silica material is negatively charged, binding occurs with high affinity and selectivity. Immobilization likely involves a high degree of molecular alignment of the enzyme, via its SBM, towards the silica surface. In contrast to silica, polymeric materials also popular in microreactor development, polydimethylsiloxane for instance, is not directly accessible, and so requires extensive surface derivatization, for enzyme immobilization.[5,11,15,31] In the current study, therefore, we made an effort to bring surface engineering for efficient SBM-enzyme immobilization into the design of silica microchannel reactors.

Coating the microchannel walls with a suitably porous silica microstructure represents a promising approach to increase the enzyme-available surface for immobilization. Among different options available, silica nanosprings as the well-characterized nanomaterials have recently gained attention in particular.[32,33] Nanosprings provide high solvent-accessible surface area and the Darcy permeability of nanosprings ($k \approx 3 \times 10^{-6}$ cm^2) demonstrates low resistance to fluid flow.[32]

Their specific surface is extremely large (~300 m^2 g^{-1}) and a plentitude of surface silanol groups are available for chemical functionalization. Similarly, these silanol groups present surface sites for enzymes to become anchored via their SBM. Using a modified vapor-liquid-solid (VLS) process, nanosprings can be deposited on essentially any solid surface able to tolerate a growth temperature of 370 °C, thus making their applications quite versatile.[34] Nanosprings were previously used as a support in immobilized enzyme microreactors.[32,33] However, lacking the advantages of SBM technology, the overall immobilization required multiple steps, including enzyme purification and surface functionalization, and involved 87% loss of active enzyme in the process. Nanospring layers of different thickness were compared, but the enzyme distribution within was not clarified.[33]

We show here that the major performance characteristics of a biocatalytic microreactor were consistently improved in immediate consequence of immobilizing the SBM-enzyme on microchannel walls coated with silica nanosprings as compared to immobilizing the same enzyme on "plain" silica walls. The immobilized enzyme activity was enhanced and the obtainable productivity was boosted accordingly. Due to increased retention of the enzyme into the nanospring layer, the operational stability of the microreactor increased. We did our evaluation using sucrose phosphorylase, a well-known transglucosidase that has important applications in glycoside and sugar phosphate synthesis.[35] We present evidence that surface coating with silica nanosprings extends significantly the current possibilities, and so addresses relevant limitations, of enzyme immobilization in microchannels. Combined with immobilization technology based on SBM, it appears broadly useful in microfluidic systems limited otherwise by the solid surface available for immobilizing the enzyme.

2. EXPERIMENTAL SECTION

2.1. Materials used

Resealable flowcells made of borosilicate glass were used. ~~Their design, fabrication and use were described elsewhere in detail.~~[36] The complete flowcell consists of a microstructured element placed into a suitably interfaced and conveniently opened and closed chip holder. Fluidic Connect Pro Resealable flowcell 4515 holder, Teflon tubings and connection parts were from Micronit Microtechnologies B.V (Enschede, NL). A New Era NE-1000 syringe pump (Next Advance, Averill Park, NY) was used to deliver the liquid flow. All chemicals were of analytical grade and reported elsewhere.[19,35]

2.2. Fabrication of the nanosprings-flowcell

2.2.1. Integration of the nanosprings in the resealable flowcell

The fabrication of the plain flowcell is the established standard process explained in previous work with detail.[36] Considering that the flowcell's bottom glass slide was conveniently used for surface derivatization. The procedure applied to attach nanosprings onto the glass surface is summarized in Figure 1. The surface was masked with Kapton tape, thus making sure that only the center area (i.e., the area eventually exposed to liquid flow inside the fully assembled flowcell) was used for growth of the nanosprings (Figure 1). The process of nanosprings growth on glass slides was described in detail before.[34] Synthesis was performed in a furnace operated at atmospheric pressure. A thin gold film prepared by sputtering on glass was used as catalyst. Nanosprings were formed by exposure to constant flows of a proprietary silicon precursor and oxygen in a nitrogen atmosphere. About 9 mg of the nanosprings, covering a surface area of ~3 cm^2 and forming a layer of 70 μm thickness, were grown on the glass slide. The coated area was then enclosed with a gasket made of perfluorinated elastomer. As shown in Figure 1, the gasket was present on a second glass

slide, which also contained the fluidic channel pattern. The glass slides were inserted into the flowcell holder and connected with Teflon tubings (250 μm inner diameter). The gasket had a thickness of 250 μm, which was compressed by about 10% on usage in the flowcell holder.

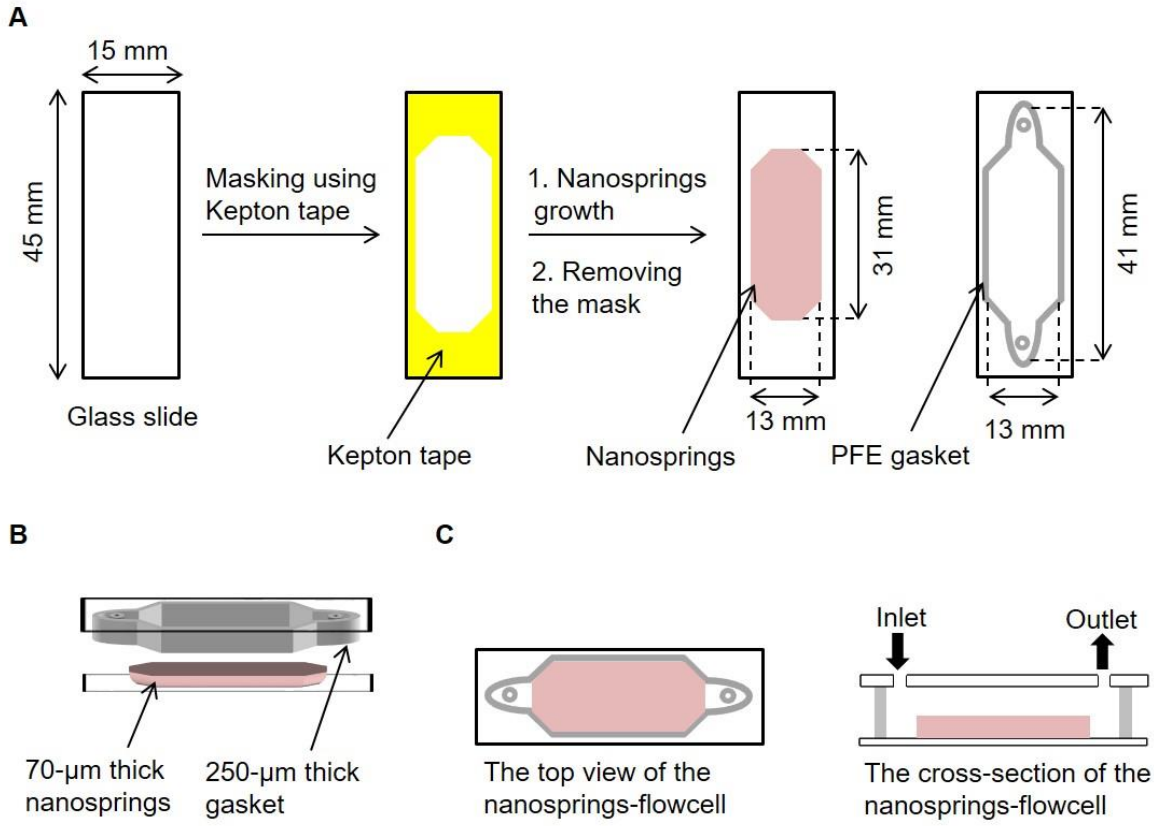

Figure 1. Preparation of the nanosprings-flowcell is shown. Panel A shows fabrication of the nanosprings glass slide. The gasket glass slide is also shown. Panel B illustrates stacking of the two glass slides on each other. Panel C shows the assembled nanosprings-flowcell (not to scale).

2.2.2. Functionalization of the nanosprings-flowcell

The nanosprings glass slide was functionalized with sulfonic acid groups (-SO_3H) using procedure from literature.[37] Glass slide was immersed in 1 M sodium hydroxide for 30 min followed by rinsing with deionized water. It was incubated in 10 % (v/v) aqueous solution of 3-(trihydroxysilyl)-1-propane-sulfonic acid for 3 h (80 °C, pH 8.0) and after that washed extensively with 50 mM potassium phosphate, pH 7.0.

2.3. Enzyme immobilization in the flowcell

2.3.1. Enzyme immobilization procedure

A chimeric form of sucrose phosphorylase from *Bifidobacterium longum* (*Bl*SPase) was used that had the binding module Z_{basic2} fused to its N-terminus. *Bl*SPase is a functional homodimer, so each enzyme chimera used here contained two Z_{basic2} modules. The enzyme is referred to as Z_*Bl*SPase throughout. Z_*Bl*SPase was produced in *Escherichia coli* BL21(DE3) as reported elsewhere.[19] Unless mentioned bacterial cell extract containing Z_*Bl*SPase was used for immobilization. The general procedure was described in earlier papers.[19,20,27] For reference from pure Z_*Bl*SPase, the enzyme was isolated according to a reported protocol[19] and shown to exhibit a specific activity of 77 U mg^{-1} of protein. One unit (U) of enzyme activity is the enzyme amount producing 1 μmol α-D-glucose 1-phosphate (αGlc 1-*P*) min^{-1} under assay conditions (25 °C, pH 7.0). The immobilization described here only briefly involved filling of the flowcell with immobilization mixture, which comprised the enzyme in 50 mM potassium phosphate, pH 8.0, supplemented with 0.25 M sodium chloride. After incubation for 2 h, the flowcell was washed with 50 mM potassium phosphate (25 °C, pH 7.0) at a flow rate (*F*) of 50 μL min^{-1}. We note, because it will be important for the discussion later, that by washing with the same phosphate buffer containing 2 M sodium

chloride, it was possible to elute the immobilized enzyme from the plain glass without causing any inactivation. Enzyme still bound to the nanosprings matrix after elution at high salt concentration (5 M sodium chloride) was removed from the nanosprings-flowcell by rinsing with 1 M hydrochloric acid and then with deionized water.

2.3.2. Measurement of the enzyme activity in solution and immobilized in the flowcell

The activity of Z_*Bl*SPase in solution and immobilized on the glass slide was measured by a spectrophotometric assay described elsewhere.[19] Briefly, the αGlc 1-*P* released on conversion of sucrose (50 mM) and potassium phosphate (50 mM) by Z_*Bl*SPase was measured as the reduced form of nicotinamide adenine dinucleotide (NADH) formed in a coupled enzymatic reaction (25 °C, pH 7.0). The NADH was determined from absorbance at 340 nm. To obtain the *apparent* activity (E_{app}) of immobilized Z_*Bl*SPase, a continuous reaction was performed in which solution of sucrose and potassium phosphate (50 mM each, 25 °C, pH 7.0) was delivered to the microreactor at different flow rates. The αGlc 1-*P* produced at steady state was measured dependent on F. E_{app} was calculated from the relationship, $E_{app} = [\alpha\text{Glc 1-}P] \times F$. It is reported in U.

2.3.3. Immobilization efficiency

Immobilization yield (Y) and catalytic effectiveness of immobilized enzyme (η) were used to characterize the efficiency of Z_*Bl*SPase immobilization in the nanosprings-SO_3^--flowcell. Y is the ratio of the enzyme activity immobilized on the surface (E_{imm}) to the total enzyme activity offered in solution (E_{tot}). E_{imm} is the difference in E_{tot} and the enzyme activity left in solution after the immobilization. Alternative way of determining E_{imm} was to elute the immobilized enzyme from the glass surface and measure its activity in solution. The latter approach was useful when

activity differences in solution were too small for a reliable determination, hence when Y was very low. η is the ratio of E_{app} to E_{imm}.

2.4. Fluorescence labeling of the immobilized enzyme

Protocol from literature was used.[29] A solution of fluorescein isothiocyanate (FITC) was prepared in dimethyl sulfoxide and diluted in 50 mM potassium phosphate, pH 7.0. The FITC solution (20 mol FITC/mol enzyme) was passed through the nanosprings-SO_3^--flowcell containing immobilized enzyme and incubated for 1 h at 25 °C. Afterwards, the flowcell was washed extensively with 50 mM potassium phosphate, pH 7.0.

2.5. Material characterization

Scanning electron microscopy (SEM) was performed with a FEI NOVA 200 dual beam system (Thermo Fisher) using secondary electron imaging at 10 keV and 130 pA with the lowest possible doses unless otherwise specified. The samples were covered with a 20-nm thick carbon layer prior to scanning.

Confocal laser scanning microscopy (CLSM) was performed using a Leica TCS SPE confocal microscope (Mannheim, Germany). The samples were excited at 488 nm, and the emission was detected in the range of 500−700 nm. A water immersion objective HCX APO LU−V-I 20×/0.50 W was used and a drop of glycerol was placed onto the nanosprings before covering the sample with a microscope coverslip. This was done to improve the match in refractive index between the medium and the nanosprings layer.

The surface area of nanosprings was determined by the Brunauer-Emmett-Teller (BET) gas adsorption method.[34]

3. RESULTS AND DISCUSSION

The shown data are from multiple independent experiments, typically three or more. Mean values were calculated from the data and are given together with the corresponding standard deviation in text.

3.1. Characteristics of the nanosprings-flowcell

The plain flowcell offered a total wall surface area of 740 mm^2, which was contributed from the top and bottom glass slides. The calculated internal volume of the flow channel was ~83 μL (Figure 1C). Note that effect of the nanosprings layer on reduction of internal volume was not considered in that value. Based on the nanosprings surface area determined by gravimetric BET (300 m^2 g^{-1}), the extra surface area introduced with the nanosprings was estimated as ~2.7 m^2.

The structure of the nanosprings coating was characterized by SEM. Analysis was performed at different positions along the glass slide using varied magnification. The complete set of SEM images recorded is given in Figure S1. SEM images from three different positions are shown in Figure 2. The overall structure of the nanosprings coating was best described as a highly irregular network of fibers arranged into a fine-mesh heterogeneous layer of material. Irregularity persisted at the level of individual nanosprings in terms of both size and shape. Nanosprings generally had strongly elongated form but differed widely in their length and thickness. Certain nanosprings had a strongly strung-out shape and appeared almost linear in shape, exhibiting only a slight internal twist. Others adopted spiral-wound conformations, differing however widely in the size of the individual coils forming the spiral. Nanosprings often displayed helicoidal shape of varying diameter (0.3 μm - 3 μm). The overall nanosprings layer exhibited non-uniform density and hence surface area, as shown in a representative cross-section image of it in Figure S2.

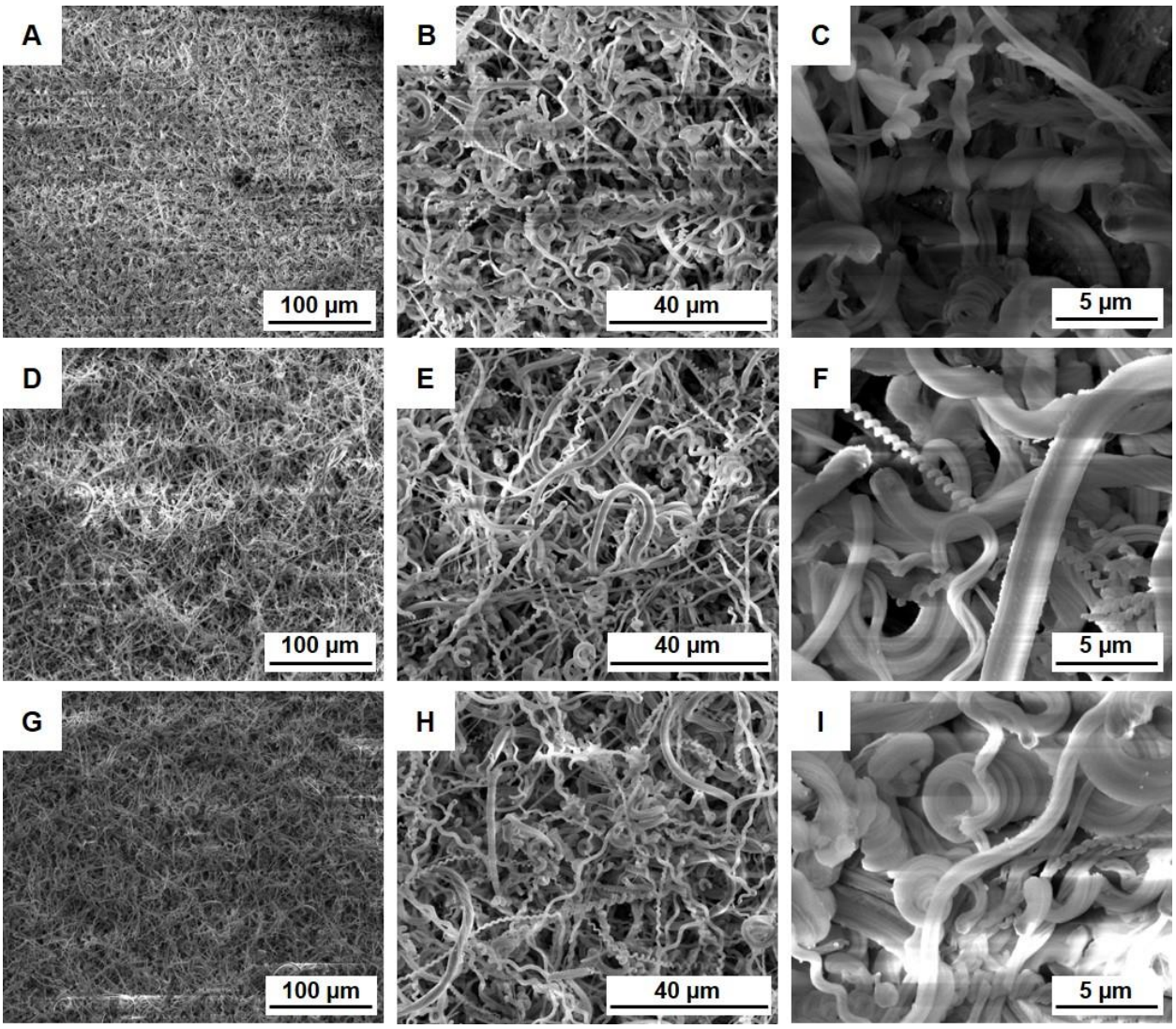

Figure 2. SEM images of the nanosprings coating are shown from three different positions on the glass slide. Each row shows one position at different magnifications.

Density increased from the surface to the bottom of the nanosprings matrix. The overall solid layer did not contain defined pores, but featured multiple interstices of variable size (from nm to µm scale). In principle, these interstices were sufficiently large to enable the enzyme (10.9 nm × 5.9 nm × 5 nm; deduced from the crystal structure of the highly similar enzyme from *Bifidobacterium adolescentis*) to penetrate the matrix by diffusion. The nanosprings layer, therefore, seemed promising for use as a densely woven, three-dimensional scaffold for Z_*Bl*SPase immobilization.

Besides offering a substantially enlarged surface area for the enzyme to become attached to, as compared to the plain surface, we also considered that the nanosprings layer might help improving the immobilization efficiency through effect on E_{app}. Although immobilization of Z_*Bl*SPase is steered mainly by the Z_{basic2} module, nonspecific protein adsorption on solid surface might occur to a limited degree, as shown in our earlier study.[19] A fibrous layer of solid material could be useful to avoid nonspecific binding of the enzyme and, in consequence, help to maximize E_{app}. We finally considered that adsorption stability of immobilized Z_*Bl*SPase might be increased on entrapment of the enzyme in the nanosprings matrix. Experiments were performed to explore these possibilities.

3.2. Performance analysis of immobilized enzyme flowcell

3.2.1. Enzyme immobilization in nanosprings-flowcells

Nanosprings-flowcells were prepared with and without surface functionalization by sulfonate groups. The surface sulfonate groups were introduced for they could potentially enhance enzyme immobilization via the Z_{basic2} module. The "plain" flowcell was used as reference. Immobilization involved offering Z_*Bl*SPase in an amount that was the same for each flowcell and exceeded by a factor of 9 the estimated maximum binding capacity of the plain surface for that enzyme (B_{max} = 2.54 μg). The Supporting Information describes the assumptions and calculations used in binding capacity assessment. It was ensured thus that enzyme in solution was not limiting the immobilization. From continuous reactor experiments performed as described in the Experimental Section, we determined the concentration of αGlc 1-*P* released at steady state (Figure 3A). Results show that the plain flowcell exhibited an E_{app} of 83±3 mU. From the value of B_{max} and the specific activity of purified Z_*Bl*SPase (77 U mg^{-1}) we calculated that the observed E_{app} corresponded to

40 % of the E_{app} expected for maximum monolayer adsorption of the enzyme on the microchannel wall, under the condition that all of the immobilized Z_*Bl*SPase was fully active (η = 1). The flowcell containing nanosprings exhibited an increase in E_{app} to 378±8 mU. The presence of sulfonate groups gave a further increase in E_{app} (583±11 mU), thus boosting the immobilization 7-fold compared to the plain reference.

Effect of varying the amount of enzyme offered (E_{tot}) on the performance of nanosprings flowcell containing sulfonate groups was studied at conditions of reactor steady state (Figure 3A). The conversions reached were up to 10-fold higher as compared to the plain flowcell. Critical parameters of the immobilization of Z_*Bl*SPase (E_{imm}, Y, η) were also determined from these experiments. Figure 3B shows that E_{imm} increased steadily on raising E_{tot}, indicating that the surface area available for immobilization was not saturated under the conditions used. Interestingly, therefore, Y was always below a value of unity ($\leq$ 0.80) that would indicate incomplete adsorption of the E_{tot} present. And, it did not change pronouncedly dependent on E_{tot} in the range used. The result suggests that, for reasons not known at the time, irrespective of the E_{tot} a certain portion ($\geq$ 20%) of the Z_*Bl*SPase present as active enzyme in solution was unable to bind to the solid surface. Considering the large increase in E_{imm} dependent on E_{tot} it was important to determine what the corresponding change in E_{app} would be. Somewhat to our surprise, a 6-fold enhancement in E_{imm} due to increase in E_{tot} was reflected in only a 1.5-fold gain in E_{app}. Therefore, this implies a dramatic decrease in η, from a value of 0.52 to one of just 0.11, in response to the increase in E_{tot}.

In the ideal case of oriented immobilization via the Z_{basic2} module in which becoming attached to the solid surface did not interfere with enzyme function in any way, η would have a value of unity,

for the immobilized enzyme (E_{app}) had exactly the same activity as the identical amount of enzyme would have in solution (E_{imm}). We have shown in earlier studies, using different Z_{basic2} chimeras of sucrose phosphorylase including Z_*Bl*SPase, that the practical upper limit of η for these enzymes immobilized on silica surface was consistently lower than 1, typically in the range 0.45 - 0.65.[19] Molecular account of η is notoriously difficult to give for immobilized enzymes, but suffice it to say that the $\eta = 0.52$ at low E_{tot} of Z_*Bl*SPase was in good agreement with literature.[19] Well-oriented enzyme immobilization via SBM technology enhanced the operational activity of immobilized enzyme up to 4-fold compared to random enzyme immobilization in nanosprings.[33] Substantial drop in η at high E_{tot} was however unexpected and only a very tentative explanation can be offered at this point. It must be emphasized for the sake of clarity that a decrease in E_{app}, and hence η, was not caused by substrate depletion or any other limitation in the experiment. At the highest E_{app} we were able to reach in continuous flow reactions (~880 mU), the substrate conversion was just around 40% when up to 90% conversion would have been possible at thermodynamic equilibrium. However, given the structure of the nanosprings matrix (Figure 2), it is conceivable that by increasing the enzyme loading, the portion of Z_*Bl*SPase localized at nano-interstices within the matrix might also increase. Due to the highly irregular network of nanowires present at these interstices, it may no longer be possible for the immobilized enzyme to have a well-defined orientation towards, and interaction with, the solid material, contrary to the more compactly organized surfaces of plain glass, like those in plates and porous beads, that exhibit a moderate or even a null curvature.[19,20,27,37] An immobilization of Z_*Bl*SPase in the nanosprings matrix that is not any more steered by the Z_{basic2} module might be responsible for the decrease in η dependent on E_{tot}. In addition, the extreme irregularity of the solid matrix and the variation in local density associated with it might hinder, more strongly than anticipated, the diffusion of even

small molecules. The possibility of diffusional limitations in supplying substrates to the immobilized enzyme could therefore not be excluded.

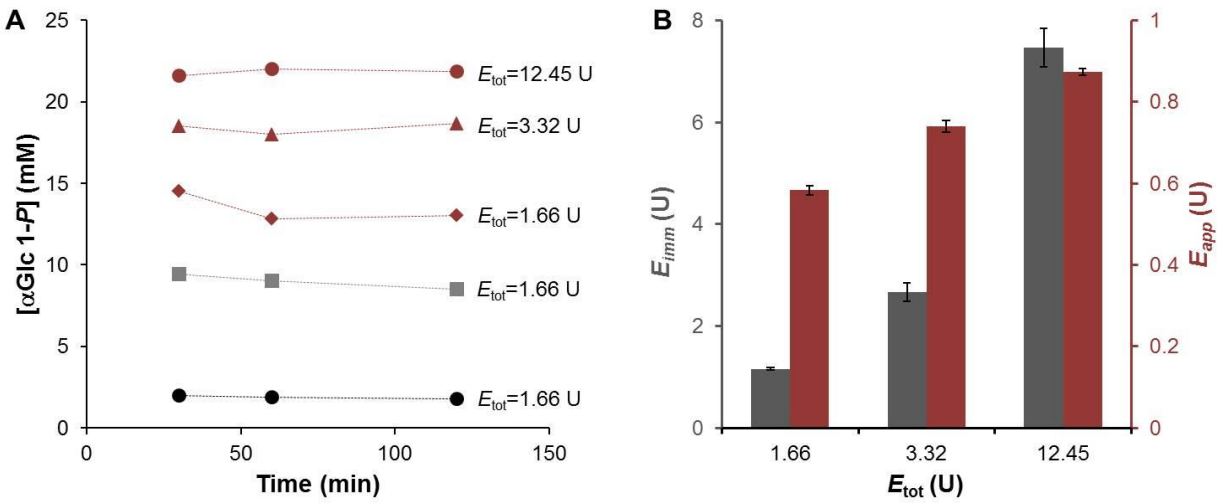

Figure 3. An analysis of immobilization in different flowcells is shown. Panel A shows the [αGlc 1-*P*] at steady state produced in continuous reactions in different flowcells (black, plain flowcell; gray, nanosprings-flowcell; red, nanosprings-SO_3^--flowcell). Panel B shows the effect of increasing the E_{tot} on the performance of the nanosprings-SO_3^--flowcell in terms of E_{imm} and E_{app}. Data in panel A are used to calculate E_{imm} and E_{app}. The conditions used were: $F = 40$ μL min^{-1}, 50 mM of each sucrose and potassium phosphate, 25 °C and pH 7.0. Results are from three independent experiments with the standard deviation of 5 %.

Using again the specific activity of the purified Z_*Bl*SPase, we calculated from the values of E_{imm} that between 15 and 100 μg of enzyme were bound onto the nanosprings-SO_3^--flowcell. These loadings are equivalent to an immobilization of 1.7 - 11 mg of protein/g of nanosprings. Compared to the B_{max} (calculated with the assumption of a strictly two-dimensional adsorption of the enzyme) normalized on the unit surface area (3.43 ng mm^{-2}), these amounts of immobilized enzyme represent a 6- to 40-fold enhancement over immobilization on the plain surface. Results show that nanosprings with a high enzyme-loading capacity significantly increase the microchannel surface.

In comparison with other surface modification techniques for enzyme immobilization such as layer-by-layer or surface-anchored polymer brushes, nanosprings coating is more easily done.[38-40]

It is evident from these considerations that immobilization of Z_*Bl*SPase in the nanosprings-SO_3^--flowcell must have involved enzyme adsorption in all three dimensions of the nanosprings matrix. However, distribution of Z_*Bl*SPase within the nanosprings layer was unknown and visualization experiments were performed for clarification.

3.2.2. Visualizing enzymes immobilized in the nanosprings-SO_3^--flowcell

Z_*Bl*SPase (15 μg) was immobilized in the nanosprings-SO_3^--flowcell, labeled fluorescently with FITC and analyzed with CLSM. Results are shown in Figure 4. A vertical cross-section image in panel A shows the nanosprings layer of about 70 μm thickness (height) on the glass surface. Close-up images (panels B - E) from different points between top and bottom of the layer are also shown. The control was a nanosprings-SO_3^--flowcell labeled with FITC but lacking the enzyme. It did not show fluorescence, thus validating the evidence in Figure 4. One recognizes immediately from Figure 4 that fluorescence was present all through the nanosprings layer, indicating that the enzyme was able to penetrate laterally and vertically, and so became distributed broadly across, the solid matrix. Images in Figure 4 (panels B - E) reveal the increase in solid matrix density on moving from top to bottom of the nanosprings layer. The nanosprings material located closer to the glass surface exhibited areas in which nanosprings were extremely strongly interwoven with relatively large interstice in between (see Figure 4E). To the extent that fluorescence intensity informs about the amount of labeled protein present locally, Z_*Bl*SPase seemed to be distributed somewhat uniformly in the nanosprings matrix irrespective of local differences in material density. The results in Figure 4 are from an immobilization of Z_*Bl*SPase that used enzyme directly from the

crude *E. coli* cell extract. To exclude the possibility of artifact, namely that FITC fluorescence in the nanosprings matrix was not from Z_*Bl*SPase but actually from another *E. coli* protein, we repeated the experiment under exactly comparable conditions but used purified Z_*Bl*SPase instead. The results are shown in Figure S3. Ability of Z_*Bl*SPase to penetrate the nanosprings layer and become immobilized in it was confirmed unambiguously.

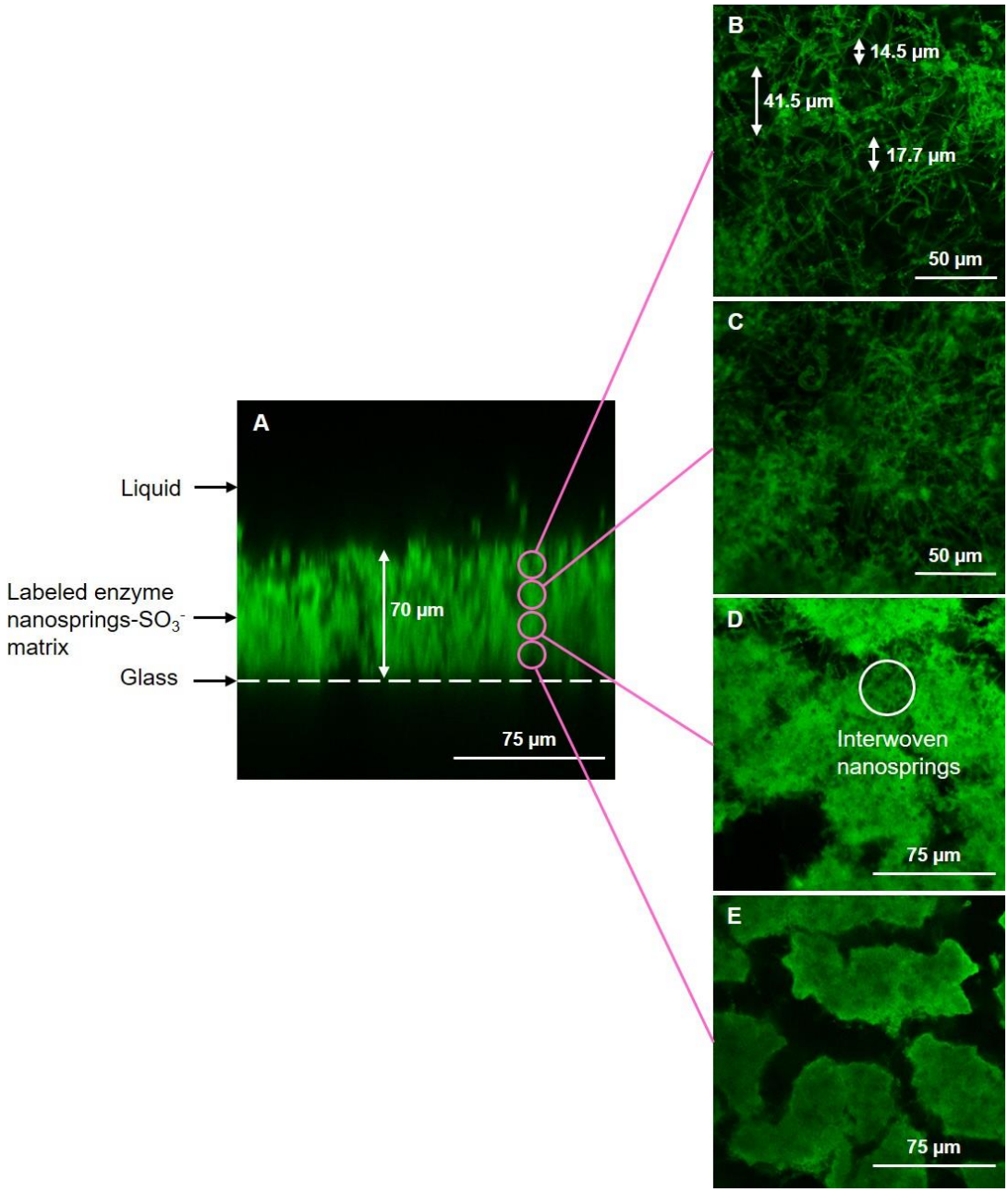

Figure 4. CLSM images of the nanosprings-SO_3^--glass slide containing FITC-labeled Z_*Bl*SPase are shown.

3.2.3. Substrate conversion in the biocatalytic microreactor dependent on liquid flow rate

Flow chemistry involves the liquid flow rate *F* as a key process variable. *F* determines the average residence time (τ_{res}) via the relationship $\tau_{res} \propto V/F$ where *V* is liquid volume of reactor. Using Z_*Bl*SPase immobilized in the nanosprings-SO_3^--flowcell, effect of *F* on substrate conversion at steady state was analyzed. Note that microreactor steady state implies time invariance of the substrate conversion at constant *F*. For each *F* used, therefore, it was ensured that steady state was maintained for a reaction time equivalent to 10 times the τ_{res}. The change in *F* was achieved via ramp-up and ramp-down of the flow rate in the range 10 - 150 μL min^{-1}. Direction of the *F* excursion, up or down, did not affect the conversions obtained. Results are summarized in Figure 5.

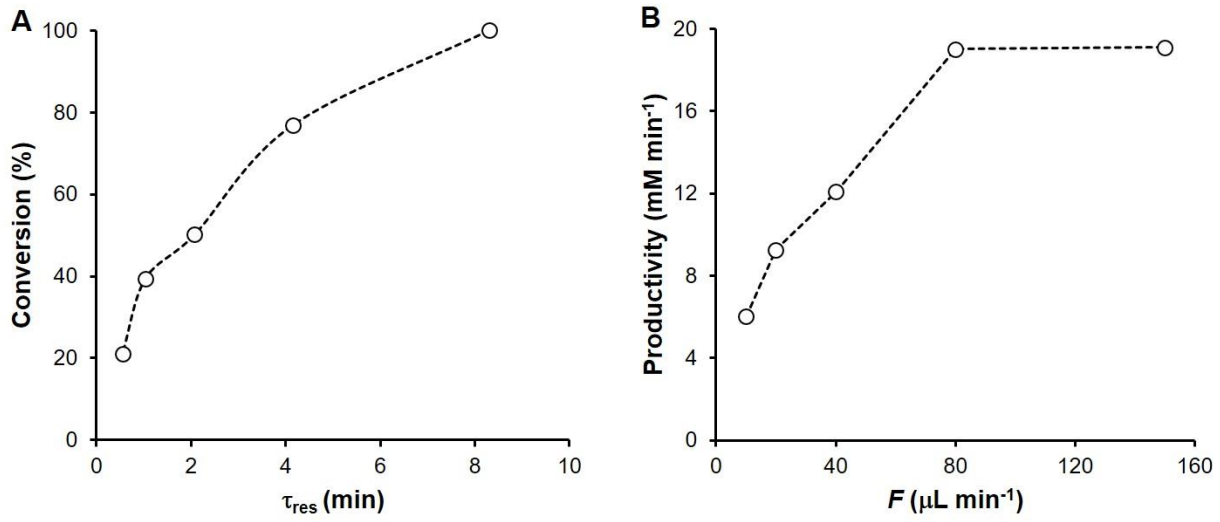

Figure 5. Performance analysis of the nanosprings-SO_3^--flowcell containing immobilized Z_*Bl*SPase (100 μg) is shown. The substrate solution contained sucrose and phosphate (50 mM of each). The concentration of αGlc 1-*P* released at steady state was measured. Conversion and productivity were calculated from the data. *F* was varied as indicated and τ_{res} calculated with a volume *V* of 83 μL. Results are from three independent experiments with the standard deviation of 5 %.

The conversion increased dependent on τ_{res}, as expected from conventional fluidic behavior of a tubular reactor, and full conversion was reached within about 8 min. The productivity increased dependent on *F* to reach a maximum at 80 μL min^{-1} or greater. Figure 5 shows that through systematic variation of *F* the microreactor performance was switched between steady states of quantitative product yield (50 mM; 100% conversion) and optimum productivity (19 mM min^{-1}) at a lower product yield of about 40%. We previously showed the productivity of 14 mM min^{-1} at the product yield of 50 % in the meander-shape fluid microchannel.[19] Higher productivity provided by nanosprings-SO_3^--flowcell, even with lower degree of miniaturization, proves the efficiency of nanosprings coating.

3.2.4. Enhanced operational stability of enzyme immobilized in nanosprings layer

Operational stability represents a critically important parameter of efficiency of the enzymatic microreactor applied to continuous flow synthesis. Enzyme immobilization via the Z_{basic2} module is readily reversible by its design. However, lacking the high endurance of enzyme immobilization via covalent fixation, its stability under continuous operation is a problem requiring special attention. Besides actual loss of enzyme activity due to denaturation under conditions of use, limited operational stability might involve effect of washing out of the enzyme. We evaluated the operational stability of immobilized Z_*Bl*SPase in time-course experiments comparing the nanosprings-SO_3^--flowcell to the plain flowcell. The reaction set-up (*F* = 40 μL min^{-1}) was selected such that the αGlc 1-*P* released at steady state was an immediate measure of E_{app}. The initial E_{app} was 874±8 mU for the nanosprings-SO_3^--flowcell while it was 83±3 mU for the plain flowcell. The actual reaction time was normalized on τ_{res} (= 2.08 min) to show the number of reactor cycles run through. The results are shown in Figure 6. Using the nanosprings-SO_3^--flowcell, about 85%

of the initial E_{app} was retained after 840 reactor cycles. Using the plain flowcell, by contrast, E_{app} decreased continuously to just 20% of the initial value after 450 reactor cycles. An operational half-life of about 269 cycles, equivalent to 560 min, was determined for Z_*Bl*SPase immobilized in the plain flowcell. The corresponding half-life of enzyme immobilized in the nanosprings-SO_3^--flowcell was approximately 6160 min, representing a substantial 11-fold enhancement of stability. Since Z_*Bl*SPase does not loose activity in the timespan of these experiments under the conditions used, the decrease in E_{app} solely reflects washing out of the immobilized enzyme. Considering previous work with the same enzyme and immobilization conditions in the meander-shape fluid microchannel, 60 % of activity was retained after the same reactor cycles.[19] Enzyme immobilization in the glass flowcell via ionic interaction showed the drastic decrease in activity to 50% after just 140 reactor cycles.[36] Enhanced operational stability of immobilized Z_*Bl*SPase is therefore ascribed to the incorporation of the enzyme into the solid matrix of nanosprings of the glass surface.

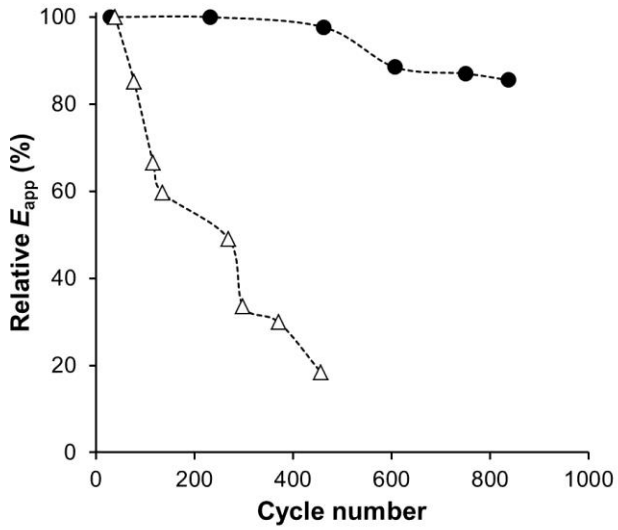

Figure 6. Comparison of nanosprings-SO_3^--flowcell (•) and plain flowcell (Δ) in terms of their operational stability is shown. Operational stability was evaluated as decrease in E_{app} over time. The total reaction time is expressed relative to the τ_{res} of 2.08 min and given as number of reactor

cycles. The conditions used were: F = 40 μL min^{-1}, 50 mM of each sucrose and potassium phosphate, 25 °C and pH 7.0. Results are from three independent experiments with the standard deviation of 8 %.

4. CONCLUSION

The current study demonstrates significant advance in enzyme immobilization in flow microchannels through well coordinated designs of the enzyme and the material used. Design of the enzyme's molecular structure as to promote efficient "affinity-like" binding to silica surfaces involved fusion to the silica binding module Z_{basic2}. Evidence for the Z_{basic2} fusion of *Bifidobacterium longum* sucrose phosphorylase herein obtained revealed that surface coating with a layer of silica nanosprings boosted the immobilization in flow microchannels in two important ways. First, enzyme binding was enhanced by an order of magnitude or more as compared to binding to the plain wall surface of uncoated microchannels. Second, resistance of the (noncovalently) bound enzyme to washing out under conditions of continuous liquid flow was also enhanced compared to the "plain surface" reference, likewise by an order of magnitude or more. The surface layer of nanosprings was characterized in its morphology as a fibrous network of material that was shown to be readily penetrated by the enzyme. The enzyme efficiency factor, which is typically quite good (≥ 0.5) for immobilizations to silica steered by the Z_{basic2} module, decreased to an unusually low value of 0.11 at high enzyme loadings into the silica nanosprings matrix. While the effect must wait further study for deeper understanding, a nanosprings synthesis mainly via lateral growth on the surface so as to lower the thickness of the final layer might help to increase the efficiency of the immobilized enzyme. Evidence from continuous reaction studies suggested that the microchannel reactor containing enzyme immobilized on nanosprings-coated wall surface is a flexible and powerful tool, for both chemistry and chemical engineering, to characterize and optimize biocatalytic transformations in flow. The operational stability of the continuous Z_*Bl*SPase reactor would enable over 1000 cycles (reactor volumes processed) to be performed with only a single load of enzyme. In summary, therefore, surface coating with silica nanosprings extends the possibilities for enzyme immobilization in flow microchannels. It

effectively boosts the performance in biocatalytic synthesis of a microstructured reactor limited otherwise by the solid surface available for immobilizing the enzyme. The optimized thickness of nanosprings layer, to diminish the diffusion limitation, might even increase the efficiency of enzyme immobilized reactors. Sufficiently large porosity of the nanosprings matrix in order for the reactor to operate at moderate pressure, provides opportunity to modify both surfaces of the flowcell with nanosprings. This would increase the productivity of reactor, albeit fabrication route optimization is needed.

ASSOCIATED CONTENT

Supporting Information. Estimation of the theoretical maximum loading of enzyme on the plain microchannel (Supporting methods). Supporting SEM images of the nanosprings-coated glass slide (Figure S1); supporting SEM image of the cross-section of the nanosprings-coated glass slide (Figure S2); supporting CLSM images showing purified enzyme immobilized in the nanosprings-SO_3^- matrix (Figure S3).

The Supporting Information is available free of charge on the ACS Publications website

at DOI:

AUTHOR INFORMATION

Corresponding Author

*Prof. Bernd Nidetzky, Institute of Biotechnology and Biochemical Engineering, Graz University of Technology, NAWI Graz, Petersgasse 12, A-8010 Graz, Austria; phone: +43 316 873 8400; fax: +43 316 873 8434; e-mail: bernd.nidetzky@tugraz.at

Present Addresses

†Experimental Biophysics and Applied Nanoscience, Faculty of Physics, Bielefeld University, 33615 Bielefeld, Germany

Author Contributions

The manuscript was written through contributions of all authors. All authors have given approval to the final version of the manuscript. DV, JMB and BN designed the research. DV performed experiments and analyzed data. MV and EXV designed and fabricated the flowcells. DNM prepared the nanosprings glass slide. DV, JMB and BN wrote the paper.

Funding Sources

European Commission; Marie Curie ITN project EUROMBR (Grant Agreement Number 608104)

ACKNOWLEDGEMENT

Dr. Zdenek Petrasek (Institute of Biotechnology and Biochemical Engineering) assisted with the CLSM experiments. Financial support from the European Commission is gratefully acknowledged. DNM acknowledges support of the United States office of Naval Research (N00014-16-1-2277).

ABBREVIATIONS

BET, Brunauer-Emmett-Teller, *Bl*SPase; sucrose phosphorylase from *Bifidobacterium longum*; CLSM, confocal laser scanning microscopy; FITC, fluorescein isothiocyanate; αGlc 1-*P*, α-D-glucose 1-phosphate; PFE, perfluorinated elastomer; SBM, silica binding modules; SEM, Scanning electron microscopy Z_*Bl*SPase; *Bl*SPase containing Z_{basic2} fused as SBM to the enzyme's N-terminus.

REFERENCES

(1) Liu, D.; Zhang, H.; Fontana, F.; Hirvonen, J. T.; Santos, H. A. Microfluidic-Assisted Fabrication of Carriers for Controlled Drug Delivery. *Lab Chip* **2017,** *17*, 1856–1883.

(2) Mauk, M.; Song, J.; Bau, H. H.; Gross, R.; Bushman, F. D.; Collman, R. G.; Liu, C. Miniaturized Devices for Point of Care Molecular Detection of HIV. *Lab Chip* **2017**, *17*, 382–394.

(3) Duncombe, T. A.; Tentori, A. M.; Herr, A. E. Microfluidics: Reframing Biological Enquiry. *Nat. Rev. Mol. Cell Biol.* **2015**, *16*, 554–567.

(4) Lei, K. F.; Huang, C.-H. Paper-Based Microreactor Integrating Cell Culture and Subsequent Immunoassay for the Investigation of Cellular Phosphorylation. *ACS Appl. Mater. Interfaces* **2014**, *6*, 22423–22429.

(5) Bhatia, S. N.; Ingber, D. E. Microfluidic Organs-on-Chips. *Nat. Biotechnol.* **2014**, *32*, 760–772.

(6) Elvira, K. S.; i Solvas, X. C.; Wootton, R. C. R.; deMello, A. J. The Past, Present and Potential for Microfluidic Reactor Technology in Chemical Synthesis. *Nat. Chem.* **2013**, *5*, 905–915.

(7) Adamo, A.; Beingessner, R. L.; Behnam, M.; Chen, J.; Jamison, T. F.; Jensen, K. F.; Monbaliu, J.-C. M.; Myerson, A. S.; Revalor, E. M.; Snead, D. R.; Stelzer, T.; Weeranoppanant, N.; Wong, S. Y.; Zhang, P. On-Demand Continuous-Flow Production of Pharmaceuticals in a Compact, Reconfigurable System. *Science* **2016**, *352*, 61–67.

(8) Gemoets, H. P. L.; Su, Y.; Shang, M.; Hessel, V.; Luque, R.; Noël, T. Liquid Phase Oxidation Chemistry in Continuous-Flow Microreactors. *Chem. Soc. Rev.* **2015**, *45*, 83–117.

(9) Wohlgemuth, R.; Plazl, I.; Žnidaršič-Plazl, P.; Gernaey, K. V.; Woodley, J. M. Microscale Technology and Biocatalytic Processes: Opportunities and Challenges for Synthesis. *Trends Biotechnol.* **2015**, *33*, 302–314.

(10) Bolivar, J. M.; Wiesbauer, J.; Nidetzky, B. Biotransformations in Microstructured Reactors: More than Flowing with the Stream? *Trends Biotechnol.* **2011**, *29*, 333–342.

(11) Laurenti, E.; dos, S. V. J. A. Enzymatic Microreactors in Biocatalysis: History, Features, and Future Perspectives. *Biocatalysis* **2016**, *1*, 148–165.

(12) Matosevic, S.; Szita, N.; Baganz, F. Fundamentals and Applications of Immobilized Microfluidic Enzymatic Reactors. *J. Chem. Technol. Biotechnol.* **2011**, *8*, 325–334.

(13) Asanomi, Y.; Yamaguchi, H.; Miyazaki, M.; Maeda, H. Enzyme-Immobilized Microfluidic Process Reactors. *Molecules* **2011**, *16*, 6041–6059.

(14) Luka, G.; Ahmadi, A.; Najjaran, H.; Alocilja, E.; DeRosa, M.; Wolthers, K.; Malki, A.; Aziz, H.; Althani, A.; Hoorfar, M. Microfluidics Integrated Biosensors: A Leading Technology towards Lab-on-a-Chip and Sensing Applications. *Sensors* **2015**, *15* 30011–30031.

(15) Sims, P. A.; Greenleaf, W. J.; Duan, H.; Xie, X. S. Fluorogenic DNA Sequencing in PDMS Microreactors. *Nat. Methods* **2011**, *8*, 575–580.

(16) Küchler, A.; Bleich, J. N.; Sebastian, B.; Dittrich, P. S.; Walde, P. Stable and Simple Immobilization of Proteinase K Inside Glass Tubes and Microfluidic Channels. *ACS Appl. Mater. Interfaces* **2015**, *7*, 25970–25980.

(17) Bolivar, J. M.; Nidetzky, B. Smart Enzyme Immobilization in Microstructured Reactors. *Chim. Oggi Chem. Today* **2013**, *31*, 50–54.

(18) de León, A. S.; Vargas-Alfredo, N.; Gallardo, A.; Fernández-Mayoralas, A.; Bastida, A.; Muñoz-Bonilla, A.; Rodríguez-Hernández, J. Microfluidic Reactors Based on Rechargeable Catalytic Porous Supports: Heterogeneous Enzymatic Catalysis via Reversible Host–Guest Interactions. *ACS Appl. Mater. Interfaces* **2017**, *9*, 4184–4191.

(19) Valikhani, D.; Bolivar, J. M.; Pfeiffer, M.; Nidetzky, B. Multivalency Effects on the Immobilization of Sucrose Phosphorylase in Flow Microchannels and Their Use in the Development of a High-Performance Biocatalytic Microreactor. *ChemCatChem* **2017**, *9*, 161–166.

(20) Bolivar, J. M.; Tribulato, M. A.; Petrasek, Z.; Nidetzky, B. Let the Substrate Flow, Not the Enzyme: Practical Immobilization of D-Amino Acid Oxidase in a Glass Microreactor for Effective Biocatalytic Conversions. *Biotechnol. Bioeng.* **2016**, *113*, 2342–2349.

(21) Bolivar, J. M.; Krämer, C. E. M.; Ungerböck, B.; Mayr, T.; Nidetzky, B. Development of a Fully Integrated Falling Film Microreactor for Gas–liquid–solid Biotransformation with Surface Immobilized O_2-Dependent Enzyme. *Biotechnol. Bioeng*. **2016**, *113*, 1862–1872.

(22) Thomsen, M. S.; Nidetzky, B. Coated-Wall Microreactor for Continuous Biocatalytic Transformations Using Immobilized Enzymes. *Biotechnol. J.* **2009**, *4*, 98–107.

(23) Tang, C.; Saquing, C. D.; Morton, S. W.; Glatz, B. N.; Kelly, R. M.; Khan, S. A. Cross-Linked Polymer Nanofibers for Hyperthermophilic Enzyme Immobilization: Approaches to Improve Enzyme Performance. *ACS Appl. Mater. Interfaces* **2014**, *6*, 11899–11906.

(24) Betancor, L.; Luckarift, H. R.; Seo, J. H.; Brand, O.; Spain, J. C. Three-Dimensional Immobilization of Beta-Galactosidase on a Silicon Surface. *Biotechnol. Bioeng.* **2008**, *99*, 261–267.

(25) Santos, J. C. S. dos; Barbosa, O.; Ortiz, C.; Berenguer-Murcia, A.; Rodrigues, R. C.; Fernandez-Lafuente, R. Importance of the Support Properties for Immobilization or Purification of Enzymes. *ChemCatChem* **2015**, *7*, 2413–2432.

(26) Hartmann, M.; Kostrov, X. Immobilization of Enzymes on Porous Silicas – Benefits and Challenges. *Chem. Soc. Rev.* **2013**, *42*, 6277–6289.

(27) Bolivar, J. M.; Nidetzky, B. Positively Charged Mini-Protein Z_{basic2} As a Highly Efficient Silica Binding Module: Opportunities for Enzyme Immobilization on Unmodified Silica Supports. *Langmuir* **2012**, *28*, 10040–10049.

(28) Jiang, Y.; Shi, L.; Huang, Y.; Gao, J.; Zhang, X.; Zhou, L. Preparation of Robust Biocatalyst Based on Cross-Linked Enzyme Aggregates Entrapped in Three-Dimensionally Ordered Macroporous Silica. *ACS Appl. Mater. Interfaces* **2014**, *6*, 2622–2628.

(29) Rocha-Martín, J.; Rivas, B. de las; Muñoz, R.; Guisán, J. M.; López-Gallego, F. Rational Co-Immobilization of Bi-Enzyme Cascades on Porous Supports and Their Applications in Bio-Redox Reactions with In Situ Recycling of Soluble Cofactors. *ChemCatChem* **2012**, *4*, 1279–1288.

(30) Denčić, I.; de Vaan, S.; Noël, T.; Meuldijk, J.; de Croon, M.; Hessel, V. Lipase-Based Biocatalytic Flow Process in a Packed-Bed Microreactor. *Ind. Eng. Chem. Res.* **2013**, *52*, 10951–10960.

(31) Zhou, J.; Ellis, A. V.; Voelcker, N. H. Recent Developments in PDMS Surface Modification for Microfluidic Devices. *Electrophoresis* **2010**, *31*, 2–16.

(32) Schilke, K. F.; Wilson, K. L.; Cantrell, T.; Corti, G.; McIlroy, D. N.; Kelly, C. A Novel Enzymatic Microreactor with Aspergillus Oryzae β-Galactosidase Immobilized on Silicon Dioxide Nanosprings. *Biotechnol. Prog.* **2010**, *26*, 1597–1605.

(33) Fu, H.; Dencic, I.; Tibhe, J.; Sanchez Pedraza, C. A.; Wang, Q.; Noel, T.; Meuldijk, J.; de Croon, M.; Hessel, V.; Weizenmann, N.; Oeser, T.; Kinkeade, T.; Hyatt, D.; Van Roy, S.; Dejonghe, W.; Diels, L. Threonine Aldolase Immobilization on Different Supports for Engineering of Productive, Cost-Efficient Enzymatic Microreactors. *Chem. Eng. J. (Amsterdam, Neth.)* **2012**, *207–208*, 564–576.

(34) Kengne, B.-A. F.; Alayat, A. M.; Luo, G.; McDonald, A. G.; Brown, J.; Smotherman, H.; McIlroy, D. N. Preparation, Surface Characterization and Performance of a Fischer-Tropsch Catalyst of Cobalt Supported on Silica Nanosprings. *Appl. Surf. Sci.* **2015**, *359*, 508–514.

(35) Goedl, C.; Schwarz, A.; Minani, A.; Nidetzky, B. Recombinant Sucrose Phosphorylase from *Leuconostoc mesenteroides*: Characterization, Kinetic Studies of Transglucosylation, and Application of Immobilised Enzyme for Production of α-D-Glucose 1-Phosphate. *J. Biotechnol.* **2007**, *129*, 77–86.

(36) Viefhues, M.; Sun, S.; Valikhani, D.; Nidetzky, B.; Vrouwe, E. X.; Mayr, T.; Bolivar, J. M. Tailor-Made Resealable Micro(bio)reactors Providing Easy Integration of in Situ Sensors. *J. Micromech. Microeng.* **2017**, *27*, 065012.

(37) Bolivar, J. M.; Nidetzky, B. Oriented and Selective Enzyme Immobilization on Functionalized Silica Carrier Using the Cationic Binding Module Z_{basic2}: Design of a Heterogeneous D-Amino Acid Oxidase Catalyst on Porous Glass. *Biotechnol. Bioeng.* **2012**, *109*, 1490–1498.

(38) Bi, Y.; Zhou, H.; Jia, H.; Wei, P. A Flow-through Enzymatic Microreactor Immobilizing Lipase Based on Layer-by-Layer Method for Biosynthetic Process: Catalyzing the Transesterification of Soybean Oil for Fatty Acid Methyl Ester Production. *Process Biochem.* **2017**, *54*, 73–80.

(39) Cullen, S. P.; Mandel, I. C.; Gopalan, P. Surface-Anchored Poly(2-Vinyl-4,4-Dimethyl Azlactone) Brushes as Templates for Enzyme Immobilization. *Langmuir* **2008**, *24*, 13701–13709.

(40) Feng, Q.; Hou, D.; Zhao, Y.; Xu, T.; Menkhaus, T. J.; Fong, H. Electrospun Regenerated Cellulose Nanofibrous Membranes Surface-Grafted with Polymer Chains/Brushes via the Atom Transfer Radical Polymerization Method for Catalase Immobilization. *ACS Appl. Mater. Interfaces* **2014**, *6*, 20958−20967.

Table of Contents